ELSEVIER

PII: S0032-3861(98)00049-4

Polymer Vol. 39 No. 19, pp. 4665–4673, 1998

0032-3861/98/$19.00+0.00

Study of the surface glass transition behaviour of amorphous polymer film by scanning-force microscopy and surface spectroscopy

Tisato Kajiyama*, Keiji Tanaka and Atsushi Takahara
Department of Materials Physics and Chemistry, Graduate School of Engineering, Kyushu University, 6-10-1 Hakozaki, Higashi-ku, Fukuoka 812-8581, Japan
(Received 25 June 1997; revised 12 November 1997; accepted 9 December 1997)

The surface molecular motion of amorphous polymeric solids has been directly measured by lateral force microscopic (LFM), scanning viscoelasticity microscopic (SVM) and differential X-ray photoelectron spectroscopic (D-XPS) measurements. SVM and LFM measurements revealed that the molecular motion on the surface of the monodisperse PS film with *M*n less than ca. 30 k was fairly active compared with that in the bulk, mainly due to the surface segregation of chain end groups. The chain end group segregation at the air/PS interface was verified by dynamic secondary ion mass spectroscopic depth profiling of the proton and deuterium ion for end-labelled PS film. These results suggest that surface T_g is depressed because of an increase in free volume near the surface region, induced by the preferential surface localization of chain end groups. D-XPS was utilized for the characterization of surface molecular motion of symmetric poly(styrene–block–methyl methacrylate) diblock copolymer [P(St-b-MMA)] films. It was confirmed by D-XPS that the surface molecular motion of the PS component in [P(St-b-MMA)] diblock copolymer films was gradually activated with decreasing depth from the air/polymer interface.

(Keywords: surface molecular motion; surface T_g; chain end localization)

INTRODUCTION

Since the free energy of polymer chains will have strong influence from interface, the depth of the surface of polymeric solids can be defined as twice the radius of gyration of polymer chain. Surface structure and surface molecular motion of polymer films play an important role in various functional applications[1,2]. In order to design a highly functionalized surface, it is necessary to control surface structure and to clarify the state of thermal molecular motion in the surface region.

The glass transition behaviour of polymer thin films has recently been paid great attention. Since the thin film has a large surface to volume ratio, the influence of the surface on the glass transition temperature, T_g might be prominent. In the case of ultrathin polymer films, spectroscopic ellipsometry[3], X-ray reflectivity[4], positron annihilation lifetime spectroscopy[5], and Brillouin scattering[6] studies have indicated that T_g may be a function of film thickness and also, depends on whether the film is free-standing or in contact with a substrate, and on the extent of polymer/substrate interaction. Depending on the extent of polymer/substrate interaction, T_g of ultrathin films increases or decreases by 50~70 K in comparison with that for a bulk region[3–6]. On the other hand, the second harmonic generation study of randomly dye-labelled polymer concluded that no change in mobility was evident[7]. However, little study has been done on the glass transition behaviour at free surfaces of bulk polymers.

The molecular dynamics simulation of atactic polypropylene on graphite predicted a decrease in density at the air/solid interface region[8]. Meyers and co-workers asked the question ''Is the surface of polystyrene really glassy?''[9]. They used atomic force microscopy (AFM) to study the wear of a PS surface and found that the outermost surface of the PS film with molecular weight less than 24 k was in a rubbery state from the recovery characteristics of the scratched pattern formed by a cantilever tip of AFM. This experiment was performed under large deformation which corresponded to a non-linear viscoelastic condition. However, no direct experimental evidence has been obtained for molecular motion in a linear mechanical response at the surface region.

The purpose of this study is to propose novel methods for the characterization of surface glass transition behaviour for thick polymer films. The surface molecular motions of the monodisperse and polydisperse polystyrenes (PSs) were studied on the basis of scanning viscoelasticity microscopy (SVM) and lateral force microscopy (LFM). In order to discuss the origin of activated surface molecular motion, the dynamic secondary ion mass spectroscopic (DSIMS) depth profiling was done for end-labelled PS. Finally, the surface molecular motion at the film surface of symmetric poly(styrene–block–methyl methacrylate) diblock copolymer [P(St-b-MMA)] was directly evaluated by differential X-ray photoelectron spectroscopy (D-XPS).

SCANNING VISCOELASTICITY MICROSCOPIC STUDIES OF SURFACE MOLECULAR MOTION FOR MONODISPERSE POLYSTYRENE FILMS

Scanning force microscopy (SFM) is one of the family of scanning probe microscopic techniques and has proven to be important for investigation of the surface morphology of

* To whom correspondence should be addressed

materials with high resolution[10]. SFM images were created on the basis of the various forces acting between cantilever tip and sample surface such as van der Waals, electrostatic, frictional, magnetic forces and so on. AFM[11] is a widely used instrument for the observation of surface topography, which is obtained by detecting the normal force acting between sample surface and probe tip. The magnitude of the modulus for the generally used silicon or silicon nitride probe tip is 200–300 GPa, which is much higher than that of the polymer surface. Therefore, when the observation is carried out in a repulsive region of the force curve, the sample surface can be deformed due to the indentation of the tip. The modulation of the tip indentation leads to the modulation of the force acting between sample surface and tip. If the modulation of the tip indentation is applied sinusoidally to the sample surface (stimulation strain), the dynamic viscoelastic properties at the sample surface can be evaluated by measuring the amplitude of the modulated response stress signal and the phase lag between modulation signal (stimulation strain) and modulated force signal (response stress)[12,13] Forced modulation AFM equipment, the so-called 'scanning viscoelasticity microscope (SVM)', was designed by remodelling a commercially available AFM[14,15]. The purpose of this section is to investigate the surface thermal molecular motion of monodisperse PS films on the basis of SVM measurement.

Table 1 shows the physicochemical properties, such as the number-average molecular weight, *M*n and the polydispersity, *M*w/*M*n, where *M*w denotes the weight-average molecular weight for the monodisperse PSs used in this study. Monodisperse PSs were prepared by a living anionic polymerization at 293 K using *sec*-butyllithium as an initiator. The magnitudes of *M*n and *M*w/*M*n were determined by gel permeation chromatography (g.p.c.) with ps standards. Bulk T_g was evaluated on the basis of differential scanning calorimetric (d.s.c.) measurement at a heating rate of 10 K min^{-1} under dry nitrogen purge. PS films ca. 200 nm thick were coated from a toluene solution onto a silicon wafer with native oxide layer by a spin-coating method. The surface dynamic viscoelastic functions of the PS films were evaluated on the basis of SVM measurement, which was performed at 293 K in air under a repulsive force of ca. 10 ~ 20 nN. A commercially available silicon nitride (Si_3N_4) cantilever with integrated tips (Olympus Co., Ltd.) was used. The nominal bending spring constant of the cantilever was 0.09 N m^{-1}. The modulation frequency and the modulation amplitude at the supporting part of the cantilever were 4 kHz and 1.0 nm, respectively.

The SFM apparatus, SPA 300 (Seiko Instruments Industry Co., Ltd.) with an SPI 3700 controller was used for surface viscoelasticity measurement[14,16]. The specimen is mounted on an XYZ piezoscanner with a 20-μm scan range which has a resonance frequency of 15 kHz. The Z-sensitivity of the piezoelectric scanner is 4.46 nm V^{-1}. The cantilever tip is mounted on the piezoelectric bimorph transducer which has a resonance frequency of 1 kHz~10 kHz depending on the magnitude of an applied electric field. The bimorph consisted of alternating layers of metal electrodes, dielectric films and piezoelectric zinc oxide films and could be bent vertically by applying opposite electric fields to the upper and lower piezoelectric sections. The cantilever position in the z-direction is modulated sinusoidally by applying an A.C. electric field, which is generated by the frequency generator, to the piezoelectric bimorph transducer. The deflection of the cantilever is measured by a position-sensitive four-segment photodiode (PSD) and feeds into the feedback loop that controls the position of the specimen. The modulated force is detected by the deflection of the cantilever. The deflection signal obtained with PSD is filtered by a band-pass filter (BPF) in order to remove high- and low-frequency noise and feeds into a two-phase lock-in amplifier. The reference signal used is the sinusoidal signal from frequency generator which corresponds to the dynamic strain signal.

The surface dynamic viscoelastic functions of the monodisperse PS film were evaluated on the basis of SVM measurement[16]. The distance between tip and sample surface was decisively influenced by the thermal drift of the piezo scanner. Thus, the measurement was carried out after attainment of thermal equilibrium. Also, in our SVM measurement, the bimorph at the other end of cantilever tip was modulated sinusoidally. Therefore, although the modulation amplitude of the bimorph could be evaluated accurately, the modulation amplitude of indentation of the cantilever tip could not be determined precisely. In order to simplify the analysis, it was assumed that the magnitude of the modulation amplitude for the tip was same as that for the bimorph actuator.

Gaub et al. derived the surface dynamic storage modulus, E' and surface loss modulus, E'' of the organic thin film on the basis of forced oscillation SFM measurement under the condition of sample stage modulation[13]. Similarly, in the

Table 1 Characterization of the monodisperse PS used in this study

*M*n	*M*w/*M*n
1.7 k	1.09
2.7 k	1.10
4.9 k	1.08
7.5 k	1.09
9.0 k	1.09
19.7 k	1.07
26.6 k	1.09
40.4 k	1.08
47.5 k	1.05
140.0 k	1.06
218.6 k	1.04
1800.0 k[a]	< 1.30

[a]Purchased from Pressure Chemical Co., Ltd

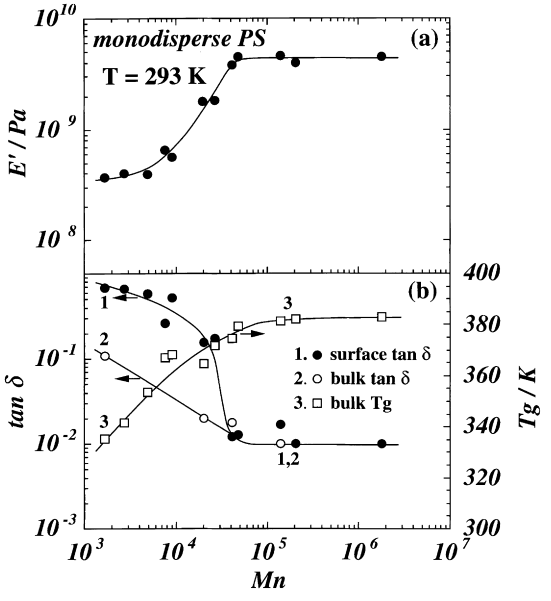

Figure 1 Molecular weight dependence of surface E' and surface tan δ for monodisperse PS films at 293 K. Bulk tan δ and bulk T_g values were evaluated by using Rheovibron and d.s.c., respectively

case of SVM measurement under the condition of cantilever modulation, if an apparent phase lag between response force and applied sample deformation, ϕ, is very small, surface E' and surface E' of the polymeric film can be expressed as follows:

$$E' = (k_c \cdot H/\gamma) \cdot \{(\cos\phi) - \gamma\} \quad (1)$$

$$E' = (k_c \cdot H/\gamma) \cdot \sin\phi \quad (2)$$

where k_c and γ are the spring constant of the cantilever along the bent direction and the amplitude ratio of response force to stimulation deformation, respectively. Also, H is a shape factor of which the magnitude is related to the contact area between sample surface and probe tip. From equations (1) and (2), the surface loss tangent, tan δ can be obtained by use of equation (3).

$$\tan\delta = E''/E' = \sin\phi/\{(\cos\phi) - \gamma\} \quad (3)$$

Since the magnitude of k_c is known and the magnitudes of ϕ and γ are obtained experimentally, the magnitudes of E' and E'' can be determined after the magnitude of H is evaluated as discussed below. The electrical and mechanical phase lags of the instruments were calibrated by using a silicon wafer as a standard with phase lag of zero.

Figure 1 shows the molecular weight dependence of surface E' and surface tan δ for the monodisperse PS films as well as the bulk tan δ and bulk T_g values[15,16]. The *M*n dependence of the output voltage as a stress signal was obtained experimentally before the determination of the magnitude of H. Since, in a higher *M*n range from 40.4 k to 1.8 M, the output voltage as a stress signal was almost constant, that is, there is no *M*n dependence on the magnitude of surface E', it seems reasonable to consider that the influence from the surface localization of chain ends is negligible with respect to the magnitude of surface E'. Especially, in the case of the PS film with *M*n of 1.8 M, since the concentration of chain end group is extremely low, it seems reasonable to assume that thermal molecular motion at the film surface is comparable with that for the bulk sample even if chain end groups are preferentially segregated at the film surface. Then, on the assumption that the magnitude of surface E' is the same that of the bulk E' at 293 K, the magnitude of H can be decided. Since the magnitudes of apparent phase lag between force and sample deformation, ϕ, and the ratio of modulation amplitude, γ, were experimentally measured, the magnitudes of surface E' and surface tan δ for the PS film with different *M*n values were evaluated by using equations (1) and (3). In a *M*n range higher than 40.4 k, the magnitudes of surface E' and surface tan δ were constant and their magnitudes were ca. 4.5 GPa and 0.01, respectively, as shown in *Figure 1*. This indicates that the surface is in a glassy state at 293 K for the PS film with larger *M*n than 40.4 k, judging from the magnitudes of surface E' and surface tan δ. Also, in the case of *M*n smaller than 26.6 k, the magnitudes of surface E' and surface tan δ decreased and increased with a decrease in *M*n, respectively. The magnitudes of surface E' and surface tan δ indicate that the surface of the PS film with *M*n lower than 26.6 k is in a glass–rubber transition state even at 293 K. Bulk dynamic viscoelastic properties of the monodisperse bulk PS sample were measured in order to compare them with the surface properties. Since, in the case of *M*n smaller than 40.4 k, the film was very fragile, the dynamic spring analysis technique was applied to evaluate bulk tan δ[17]. In the case of *M*n smaller than 26.6 k, the magnitude of surface tan δ was much higher than that of bulk tan δ, as shown in *Figure 1*. The absence of entanglement at *M*n $<$ 26.6 k would imply that any work done in deforming the surface would be accompanied by mechanical loss. AFM observation revealed that the surface was smooth after SVM measurement. The absence of permanent irreversible deformation after measurement indicates that the SVM was done under reversible deformation conditions. Thus, it can be concluded that the activation of surface molecular motion occurred at *M*n less than 26.6 k. These results clearly indicate that the surface T_g of the PS film is more strongly dependent on *M*n than the bulk T_g, because the chain end effect on surface tan δ is more apparent than that on bulk tan δ.

LATERAL FORCE MICROSCOPIC STUDIES OF SURFACE MOLECULAR MOTION FOR MONODISPERSE POLYSTYRENE FILMS

LFM is a useful tool for scanning rate- and temperature-dependent two-dimensional measurements of lateral force, which is evaluated by detecting the torsion of the sliding cantilever[18]. Since the force measured by LFM is the sum of frictional and adhesion forces acting between sample surface and cantilever tip[19], the term LFM is used instead of 'frictional force microscopy' in this paper. Since the frictional behaviour of polymeric solids is closely related to their dynamic viscoelastic properties[20], it is possible to investigate the surface molecular motions of the polymeric solids by using LFM which can detect lateral force between solid surface and sliding cantilever tip on nanometer scale[16,21]. The scanning rate-dependence of the lateral force corresponds to the frequency dependence of the loss modulus, E''. In the cases of the glassy surface or rubbery one, no distinct scanning rate-dependence of lateral force is observed. Whereas, in the case of the surface in a glass–rubber transition state, the maximum peak of frictional force with the scanning rate is generally observed due to an appearance of the E'' maximum in a transition region. Therefore, when the magnitude of lateral force evaluated by

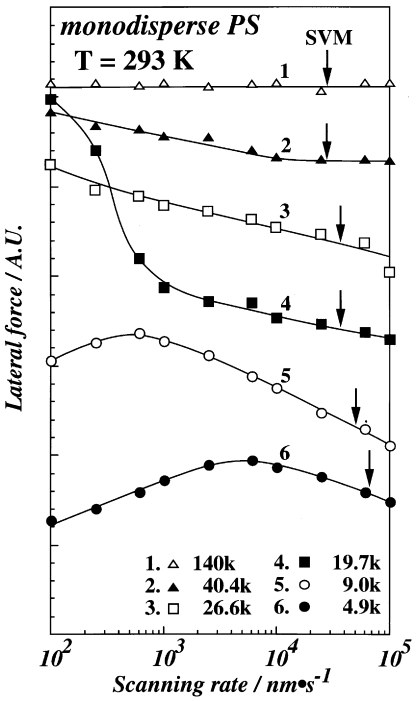

Figure 2 Scanning rate-dependence of lateral force for the monodisperse PS films at 293 K as a function of *M*n

LFM exhibits apparent scanning rate-dependence, it can be concluded that the surface is in a glass–rubber transition state.

In order to investigate the molecular weight-dependence of the surface molecular relaxation behaviour for the monodisperse PS film, the scanning rate-dependence of lateral force was measured at 293 K in air under a repulsive force of ca. 25 nN. The cantilever used for LFM measurement was the same as that used for SVM measurement. The magnitude of lateral force was evaluated by a line scan mode.

Figure 2 shows the scanning rate-dependence of lateral force as a function of *M*n of the monodisperse PS film[16]. The tip indent depth evaluated by Hertz's elastic theory[22] was ca. 1.1 nm[16]. Also, the scanning rate, ν of LFM measurement can be converted to the frequency, f of SVM measurement based on Hertz's elastic theory as given by equation (4).

$$\nu = 2f \left[\frac{3}{4} \left(\frac{1-\mu_{\text{tip}}^2}{E_{\text{tip}}} + \frac{1-\mu_{\text{polymer}}^2}{E_{\text{polymer}}} \right) RF_{\text{c}} \right]^{1/3} \quad (4)$$

where μ, E, R and F_{c} are the Poisson ratio, modulus, the radius of curvature of the tip, and contact force, respectively[16]. The broken arrows in *Figure 2* denote the scanning rates corresponding to the frequency of SVM measurements which were calculated by use of equation (4). Since no distinct scanning rate-dependence of lateral force was observed in the case of *M*n of 140 k, it seems reasonable to consider that the surface is in a glassy state. On the other hand, the magnitude of lateral force for the monodisperse PS film surface with *M*n less than 40.4 k was dependent on the scanning rate. In the case of *M*n of 40.4 k, although the scanning rate-dependence of lateral force was not observed at a high scanning rate region, lateral force increased with a decrease in the scanning rate at a low scanning rate region. This result indicates that the surface of the monodisperse PS film with *M*n of 40.4 k is clearly in a glass–rubber transition state and a glassy one at low and high scanning rate regions, respectively. In the case of *M*n of 26.6 k and 19.7 k, since lateral force continuously increased with a decrease in the scanning rate, it can be concluded that the surface is in a glass–rubber transition state at 293 K. Moreover, in the case of *M*n of 9.0 k and 4.9 k, the peak was clearly observed on the lateral force–scanning rate curve. This indicates that the surface E'' might exhibit the peak at the frequency range corresponding to the scanning rate employed in this study. That is, the surface of the monodisperse PS film with *M*n of 9.0 k and 4.9 k is already in a glass–rubber transition state at 293 K, even though the bulk T_{g} is around 360 K as shown in *Table 1*. Since the surface T_{g} for the monodisperse PS film with *M*n of 9.0 k is higher than that for *M*n of 4.9 k, it is reasonable that the peak on the lateral force–scanning rate curve for the monodisperse PS film with *M*n of 9.0 k appears in a lower scanning rate region in comparison with that for *M*n of 4.9 k. Also, it should be noticed that annealing treatment did not influence the lateral force *versus* scanning force behaviour. The above-mentioned LFM results agreed well with SVM ones if the scanning rate of the cantilever tip for LFM measurement was converted to the vibration frequency of cantilever for SVM measurement.

As shown in *Figure 1*, the magnitude of surface E' decreases with a decrease in *M*n and also, in general, that decreases with an increase in measuring temperature. Therefore, from the point of view of the variation of surface E', the *M*n dependence of surface E' at 293 K qualitatively corresponds to the measuring temperature dependence of surface E' by using the monodisperse PS film with a certain *M*n. Then, it seems reasonable to consider that a master curve based on scanning rate–lateral force superposition can be obtained from *Figure 2*, this is similar to a master curve based on time–temperature superposition. *Figure 3* shows the schematic representation of the scanning rate-dependence of lateral force for the monodisperse PS films with different *M*n values at 293 K. *Figure 3* suggests that the lateral force–scanning rate master curve can be drawn on the basis of the lateral force measurement for the monodisperse PS films with various *M*n at a fixed temperature of 293 K.

TEMPERATURE DEPENDENCE OF SURFACE MOLECULAR MOTION BY USE OF LATERAL FORCE MICROSCOPY

The scanning rate of our LFM measurement is in a range from 10^2 nm s^{-1} to 10^5 nm s^{-1}. It is impossible to obtain the lateral force–scanning rate curve on the whole range of scanning rate at a certain measuring temperature, such as 293 K. Then, the scanning rate-dependence of lateral force was evaluated at various temperatures in order to apply the time–temperature superposition principle. The scanning stage of the LFM was heated to a fixed measuring temperature under vacuum. The piezoscanner was thermally insulated from the heating stage. LFM measurements in a temperature range above 293 K were carried out in vacuo in order to avoid surface oxidation and a capillary force effect induced by surface-adsorbed water. The double gold coated cantilever used in this study has a bending spring constant of 0.09 N m^{-1}.

Figure 4 shows the scanning rate-dependence of lateral force as a function of temperature for the monodisperse PS film with *M*n of 140 k[23]. In the temperature range 293 K to 333 K, the scanning rate-dependence of lateral force was not observed. This may indicate that the surface T_{g} of the monodisperse PS film with *M*n of 140 k is higher than 333 K. On the other hand, in a temperature range from 343 K to 353 K, the magnitude of lateral force increased with a decrease in the scanning rate, especially at a lower scanning rate region. The scanning rate at which the magnitude of lateral force starts to increase with a decrease in the scanning rate was shifted to the higher scanning rate with an increase in measuring temperature from 343 K to 363 K. The existence of the scanning rate-dependence of lateral force clearly indicates that the surface is in a glass–rubber transition state at a lower scanning rate region. Since

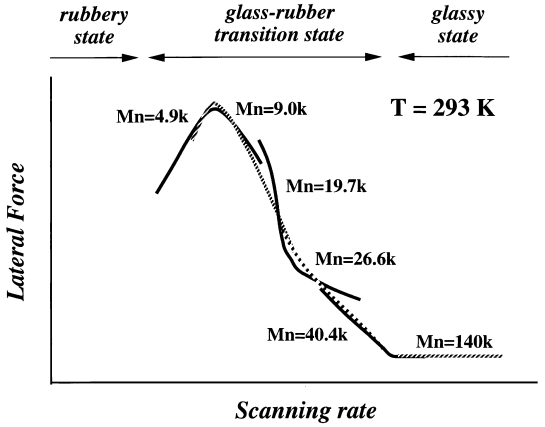

Figure 3 Schematic representation of lateral force–scanning rate curve for monodisperse PS films with different *M*n at 293 K

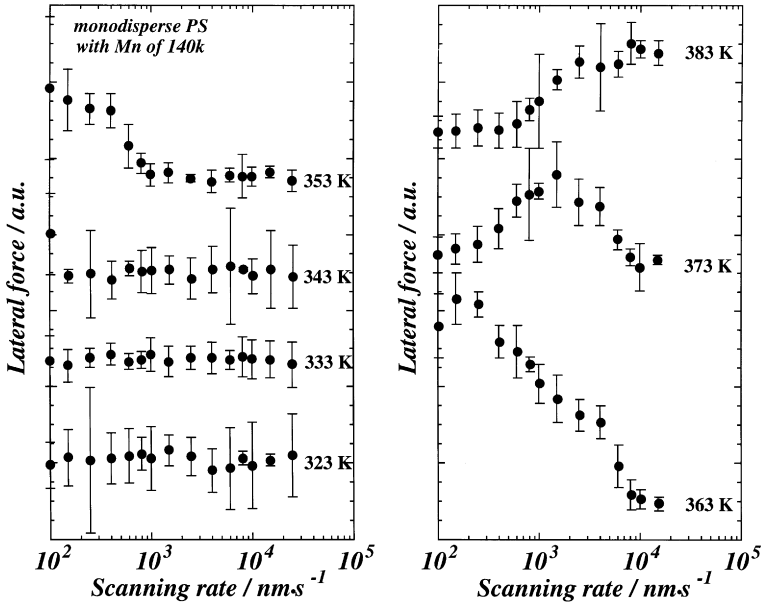

Figure 4 Scanning rate-dependence of lateral force for the monodisperse PS film with *M*n of 140 k as a function of temperature

the bulk T_g of PS with *M*n of 140 k evaluated by d.s.c. was 381.5 K, it can be concluded that the surface T_g was depressed compared with the bulk one even though the molecular weight of the monodisperse PS is so high as 140 k. Also, in the temperature range 363 K to 383 K, a distinct peak was observed on the scanning rate–lateral force curve. At 383 K above bulk T_g, the magnitude of lateral force decreased in a wide scanning rate region with a decrease in the scanning rate.

Figure 5 shows the master curve drawn by horizontal and vertical shifts of each curve shown in *Figure 4* with $T =$ 363 K as the reference temperature. The horizontal shift factor, a_T was expressed as an Arrhenius type equation in this temperature range. Since the absolute value of lateral force is very difficult to obtain, the vertical shift was also done for the construction of master curve. The shape of master curve is very similar to the frequency dependence of loss modulus or mechanical loss tangent. It seems reasonable to consider that the scanning rate-dependence of lateral force exhibits the maximum peak in a glass–rubber transition and also that is not observed in a glassy region and a rubbery one. The activation energy of surface α-relaxation evaluated from the temperature dependence of shift factor was ca 220 kJ mol^{-1}, which is lower than that observed for bulk dynamic viscoelastic measurement. This result suggested the activation of thermal molecular motion at the surface region.

DEPTH PROFILE OF CHAIN END GROUPS BY DYNAMIC SECONDARY ION MASS SPECTROSCOPY

A depression in T_g at the film surface compared with that for the bulk sample has been explained by the surface localization of chain end groups[24–26]. However, the relationship between surface localization of chain end groups and activated or enhanced surface molecular motion has not been experimentally confirmed. Deuterated polystyrene (dPS) in which the chain end groups were labelled by protonated groups was prepared by a living anionic polymerization. Depth profiling of the deuterated polystyrene (dPS) film was carried out by using dynamic secondary ion mass spectroscopic measurement (DSIMS, SIMS 4000, Seiko Instruments Inc., Atomika Analysetechnik GmbH) in order to confirm the surface localization of chain end groups. The incident beam of oxygen ions with 3.0 kV and 6~7 nA was focussed onto a 100 μm $\times$ 100 μm area of the specimen surface. A platinum layer 10 nm thick was sputter-coated on the surface of the end-labelled dPS film in order to avoid a charging up of the specimen during the DSIMS measurement.

Figure 6 shows the typical SIMS depth profile of the end-labelled dPS film[15,16]. The dashed vertical line corresponds to the air/polymer interface. The steady-state etching proceeded during the etching process. The instrumental resolution function was not corrected for the depth profile measurement due to the difficulty of evaluation. The intensity of the carbon ion, C^+ was almost constant at any depth position from the polymer film surface. Although, in general, the secondary ion efficiency of hydrogen atom is higher than that of heavy hydrogen atom, the stronger intensity of deuterium ion, D^+ than that of proton, H^+ was maintained during the etching of the polymer film. This stronger intensity of D^+ results from the larger fraction of heavy hydrogen atom in the end-labelled dPS. *Figure 6* revealed an apparent increase in the intensity of H^+ and a decrease in that of D^+ in the air/polymer interface region. Since the styrene unit was deuterated and protons were present only in both chain end portions, the SIMS depth

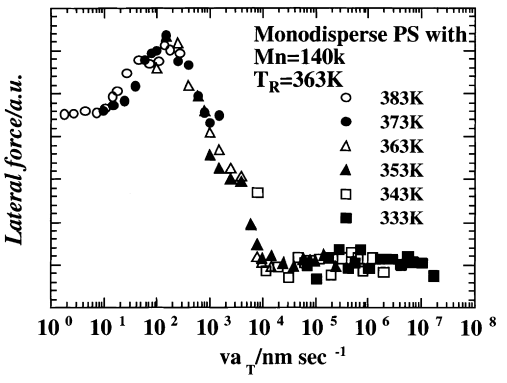

Figure 5 Master curve drawn by horizontal and vertical shifts of each curve shown in *Figure 4*. Reference temperature is 363 K

profile shows a remarkable enrichment of chain end groups at the air/polymer interface. Since the surface localization of chain end groups induces the excess free volume fraction at the film surface compared with that in the bulk phase, the surface T_g is lower than the bulk T_g, meaning that surface molecular motion at the film surface is fairly active in comparison with that for the bulk sample at room temperature, 293 K. The localization decay length of chain end groups was defined as the range from the air/polymer interface to the depth that the initial slope of H^+ profile crossed the bulk intensity. The localization decay length of chain end groups was 4.4 nm and its value was almost comparable to the radius of gyration of an unperturbed chain, *R*g of 3.3 nm.

SURFACE MOLECULAR MOTION OF POLYDISPERSE PS FILMS BY LATERAL FORCE MICROSCOPY

As mentioned above, it has been revealed that the surface of the monodisperse PS film is in a glass–rubber transition state even at 293 K, especially in the case of lower *M*n than about 30 k, since the chain end groups is localized at the air/polymer interface due to lower surface free energy of the chain end group. Here, the surface molecular motion of the polydisperse PS film, that is quite important for industrial applications, will be discussed.

Table 2 lists the physicochemical properties *M*n, *M*w/*M*n and the bulk T_g for the polydisperse PS used in this study. Those polydisperse PSs were commercially available. *Figure 7* shows the scanning rate-dependence of lateral force for the commercially available Polydisperse 1 film at 293 K[27,28]. The filled circles, the open ones and the filled squares show the results for the as-cast Polydisperse 1 film, the annealed ones at 393 K and at 423 K for 24 h, respectively. In the case of the as-cast Polydisperse 1 film, the scanning rate-dependence of lateral force was not apparent at higher scanning rate than 6×10^2 nm s^{-1} and lateral force slightly increased with a decrease in the scanning rate at a lower scanning rate than 6×10^2 nm s^{-1}. This indicates that, at lower scanning rate region, the surface is in an initial stage of a glass–rubbery transition even at 293 K. The magnitudes of surface E' and surface tan δ for the as-cast Polydisperse 1 film evaluated by SVM measurement at 293 K were 4.4 GPa and 0.02, respectively, indicating a glassy state at a corresponding scanning rate

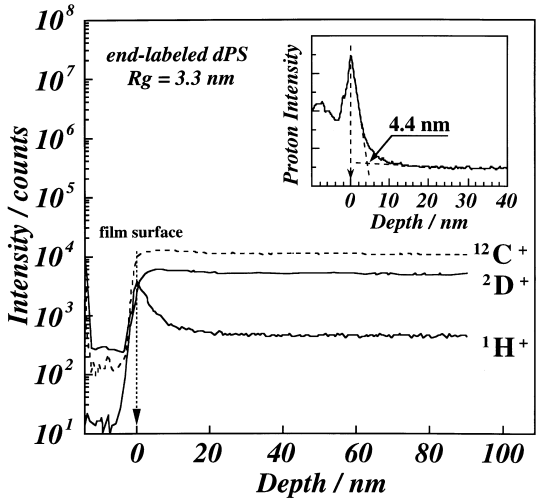

Figure 6 SIMS depth profile of the end-labelled dPS film. The inset shows the enlarged proton intensity profile in linear scale in the vicinity of the film surface

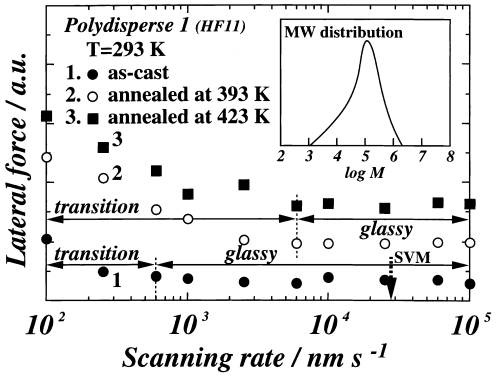

Figure 7 Scanning rate-dependence of lateral force for the commercially available Polydisperse 1 film at 293 K

shown by the arrow. When the annealing treatment of the Polydisperse 1 film was carried out at 393 K and 423 K for 24 h, the scanning rate-dependence of lateral force became more distinct up to 2.5×10^3 nm s^{-1}. As shown in *Figure 7*, the scanning rate–lateral force curve of the film annealed at 423 K are very similar to the one annealed at 393 K. Therefore, these results indicate that, when the annealing treatment of the Polydisperse 1 film was performed, the lower molecular weight components were preferentially segregated at the film surface due to lower conformational entropy difference between at the surface and in the bulk region, and also the annealing effect was almost same at the annealing temperature above bulk T_g. Even though fairly high fraction of the lower molecular weight component with *M*n lower than ca. 30 k was contained in the Polydisperse 1 system, the scanning rate-dependence of lateral force corresponding to a glass–rubber transition state was not distinct in the higher scanning rate region in comparison with that for the monodisperse PS film with corresponding *M*n of 26.6 k. The difference for the scanning rate-dependence of lateral force between monodisperse PS and polydisperse one might be explained on the basis of the difference in chemical structure of chain end groups. If the chain end group has lower surface free energy compared with the main chain part, the chain end group is preferentially localized at the film surface[29]. In the case of the PS prepared by living anionic polymerization using *sec*-butyllithium as an initiator, both chain end groups are butyl group and repeating unit, respectively. In this case, since the magnitudes of the surface free energy for the chain end groups are smaller than that of the main chain, chain end groups are preferentially segregated at the film surface[29]. Whereas, in the case of the PS prepared by radical polymerization using azobisisobutyronitrile, redox initiator and so on, the hydrophilic fragments are incorporated into the chain ends because the polymerization reaction is terminated completely by recombination. Then, since the chain end group has higher surface free energy in comparison with the main chain part, the chain end groups might migrate into a deeper surface region from the air/polymer interface. Even if the lower molecular weight component is preferentially segregated at the film surface in the case of the polydisperse PS, the end group concentration did not increase effectively at the film surface

Table 2 Characterization of the polydisperse PSs used in this study

Sample	M_n	M_w/M_n	T_g (/K)	Remarks
Polydisperse 1	29 k	6.26	375.5	HF11
Polydisperse 2	169 k	2.67	377.8	US305

from the view point of the activation of surface thermal molecular motion. Therefore, in the case of the Polydisperse PS film prepared by radical polymerization, the remarkable activation of surface molecular motion is not detected due to the preferential migration of chain end groups into a deeper surface region from the air/polymer interface, in contrast to the case that the surface molecular motion for the monodisperse PS is strikingly activated due to the preferential segregation of the chain end groups.

The Polydisperse 1 film has oligomer-like shorter chain component with Mn less than 1.5 k, of which Rg is comparable and/or less than ca. 1 nm, as shown in *Figure 7*, whereas, when the load of 25 nN was applied to tip, the indentation depth of tip calculated from the Hertz elastic theory, is ca 1.1 nm[16]. Thus, the shorter chain existing at the surface can be easily removed by the sliding tip. Therefore, even though the chain end groups does not segregate at the surface, the surface mobility becomes remarkable if the oligomer-like shorter chain is enriched at the surface.

Figure 8 shows the scanning rate-dependence of lateral force for the Polydisperse 2 film at 293 K[27,28]. The filled and the open circles show the scanning rate-dependence of lateral force for the as-cast Polydisperse 2 film and the annealed one at 393 K for 24 h, respectively. In both cases, any distinct scanning rate-dependence of lateral force was not observed, because the fraction of the lower molecular weight component is very low. Also, the magnitudes of surface E' and surface tan δ for the as-cast Polydisperse 2 film based on SVM measurement at 293 K were 4.3 GPa and 0.02, respectively. The LFM and SVM measurements indicate that the surface of the Polydisperse 2 film is in a glassy state at 293 K. Therefore, it can be concluded that if the fraction of the lower molecular weight component than 30 k is very low in spite of the broader molecular weight distribution, the surface molecular motion is not activated at room temperature because the concentration of surface-localized chain end group is negligibly low with respect to the activation of surface thermal molecular motion.

SURFACE GLASS TRANSITION TEMPERATURE OF DIBLOCK COPOLYMERS BASED ON X-RAY PHOTOELECTRON SPECTROSCOPY

In order to evaluate directly the surface molecular motion at the polymeric solid surface, the surface reorganization process for the P(St-b-MMA) copolymer film with annealing treatment was investigated in situ by D-XPS measurement[30,31]. Since the surface reorganization required polymer chain diffusion which can occur above T_g, the change in surface composition might reflect T_g at the surface region. As the acquisition time of XPS takes 10 to 15 min, the slow dynamic process of surface reorganization can be analysed in situ by XPS.

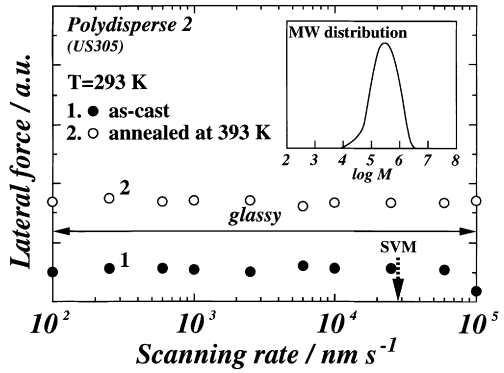

Figure 8 Scanning rate-dependence of lateral force for the Polydisperse 2 film at 293 K

The symmetric P(St-b-MMA) copolymer with Mn of 45.5 k and Mw/Mn of 1.10 was purchased from Polymer Laboratories Co. Ltd. The magnitudes of surface free energy for PS and PMMA at 298 K are 40.7 and 41.2 mJ m^{-2}, respectively[32]. The copolymer thin film with thickness of ca. 50 nm was prepared onto a gold-coated silicon wafer by a dip-coating method. d.s.c. was used to evaluate T_g of the bulk P(St-b-MMA) copolymer. The surface chemical composition of the P(St-b-MMA) film was investigated on the basis of XPS measurement. The XPS spectra were obtained with ESCA 750 X-ray photoelectron spectrometer (Shimadzu Co. Ltd.). The XPS measurement was performed under conventional conditions with an MgKα X-ray source. The analytical depth of XPS, d from the outermost surface is defined by

$$d = 3\lambda\sin\theta \tag{5}$$

where λ is the inelastic mean-free path for a photoelectron in the solids and θ is emission angle of photoelectron[30]. The magnitude of d of polymeric materials ranges from 2.7 to 10.5 nm by using the value of λ evaluated from Ashley's equation[33]. The surface composition change owing to the annealing-induced surface reorganization process was measured by using XPS with a temperature-controlled heating stage. The annealing of the specimen was carried out from 293 K to 373 K, which was far below the ceiling temperature of PMMA, at 5 K intervals. The specimen was held at each temperature for 8 h.

The d.s.c. thermogram of the P(St-b-MMA) film showed two baseline shifts which indicated two T_gs. This result indicates that the bulk P(St-b-MMA) is in a microphase-separated state of the PS and the PMMA components. The temperature at the midpoint of the base line shift was defined as T_g. In comparison with the PS and PMMA homopolymers it was revealed that the lower and the higher T_gs for the P(St-b-MMA) film corresponded to the PS and PMMA components, respectively. $T_{g,PS}$ and $T_{g,PMMA}$ for the bulk P(St-b-MMA) with Mn of 45.5 k were 380.5 K and 394.2 K, respectively.

The as-cast film of P(St-b-MMA) formed randomly oriented microphase-separated domains at the surface region; when the solvent was evaporated fairly fast from a solution before attainment of an equilibrium state, P(St-b-MMA) molecular chains were frozen in a non-equilibrium state. Low-voltage field-emission scanning electron microscopic observation for the as-cast P(St-b-MMA) film revealed the presence of randomly oriented domains on the film surface[34]. With an increase in annealing temperature for the as-cast P(St-b-MMA) film, the reorganization at the film surface effectively proceeded, especially after the annealing temperature reached the surface T_g and finally, the well-defined lamellar structure parallel to the film surface was formed in a quasi-equilibrium state.

Figure 9 shows the XPS C1s spectra of the as-cast P(St-b-MMA) film and also, the PS and the PMMA homopolymer ones. The C_{1s} spectra for the P(St-b-MMA) films were curve-fitted to the four peaks corresponding to neutral carbon (285.0 eV), ether carbon (286.5 eV), carbonyl carbon (288.8 eV) and the shake-up of $\pi-\pi^*$ of benzene ring (291.5~292.0 eV) by a standard non-linear curve-fitting. Then, the surface PS weight fraction, ω was evaluated by using equation (6).

$$\frac{I_{C=O}+I_{C-O}}{I_{total}} = \frac{2(1-\omega)/M_{MMA}}{\omega/M_S + 5(1-\omega)/M_{MMA}} \tag{6}$$

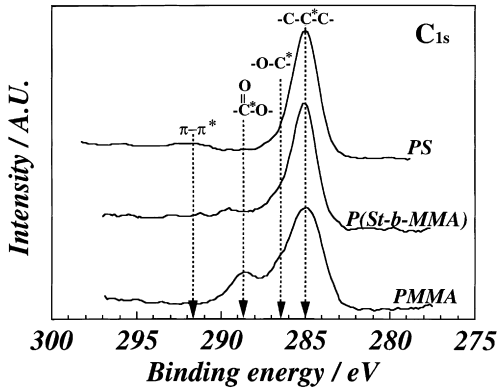

Figure 9 The XPS C_{1s} spectra of the as-cast P(St-b-MMA) film and also, PS and PMMA films

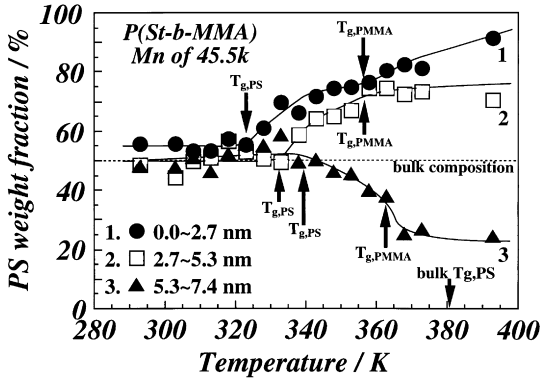

Figure 10 The annealing temperature-dependence of surface composition of the P(St-b-MMA) film as a function of the analytical depth

where I_i is the integrated intensity of a core-electron photoemission spectrum, and also M_S and M_{MMA} are the molecular weights for styrene and methyl methacrylate monomer units, respectively.

Figure 10 shows the variations of the surface PS weight fraction at different analytical depths for the P(St-b-MMA) film with *M*n of 45.5 k with annealing temperature[25,26]. The surface composition in the range of 2.7∼5.3 nm and 5.3∼7.4 nm were calculated on the basis of D-XPS measurements[25,26]. Since the initial PS weight fraction at all analytical depth was ca. 50%, it was apparent that both PS and PMMA domains were almost equally present in the surface region of 7.4 nm deep, maybe due to the formation of randomly oriented structure as discussed above. In the case of the analytical depth ranges of 0.0∼2.7 nm and 2.7∼5.3 nm, the enrichment of PS segments was recognized with an increase in annealing temperature. The enrichment of PS segments started at a certain annealing temperature, $T_{g,PS}$ as shown by the arrows in *Figure 10*. This surface enrichment of PS segments occurs in order to minimize the air/polymer interfacial free energy. On the other hand, the enrichment of PMMA segments was discernible above a certain annealing temperature in the case of the analytical depth range of 5.3∼7.4 nm. Therefore, each enrichment of PS and PMMA segments in the depth ranges of 0.0∼5.3 nm and 5.3∼7.4 nm definitely indicates the formation of the second PMMA layer beneath the first PS surface layer, since a symmetric diblock copolymer was used as the sample.

The surface reorganization can be attained in the annealing temperature range at which PS or PMMA segments can change their conformation or aggregation state in a large scale, that is, their micro-Brownian motions start. Therefore, the first and the second increases in the PS weight fraction as shown in *Figure 10* correspond to T_gs of PS and PMMA segments, because the PS and PMMA segments are present on the surface of the as-cast film. *Table 3* summarizes T_gs for the P(St-b-MMA) film in the different depth ranges. *Table 3* indicates that T_gs of PS and PMMA segments at the film surface are much lower than those for the bulk PS and PMMA samples. The magnitude of T_g decreased more strikingly as the analytical region became closer to the outermost surface. Our result seems to disagree with that of Russell et al. on the surface relaxation of rubbed PS films using near edge X-ray absorption fine structure (NEXAFS)[35]. They reported that full relaxation of the rubbed PS surface was found for temperature above bulk T_g. We are now trying to observe surface T_g directly on the basis of temperature dependence of surface modulus and tan δ.

Table 3 T_g for the P(St-b-MMA) with *M*n of 45.5 k film in the different depth ranges: T_gs for the P(St-b-MMA) diblock copolymer film with *M*n of 45.5 k in the different depth ranges

Depth range (/nm)	$T_{g,PS}$ (/K)	$T_{g,PMMA}$ (/K)
0.0∼2.7	322.5	356.5
2.7∼5.3	332.5	356.5
5.3∼7.4	339.4	362.5
Bulk	380.5	394.2

CONCLUSION

Activation of thermal molecular motion at the surface of amorphous polymeric solids has been confirmed by various experimental techniques. The SVM and LFM measurements for the monodisperse PS films and the polydisperse PS ones were carried out in order to investigate the surface molecular motion. It was revealed that the monodisperse PS film surface with *M*n less than ca. 30 k was in a glass–rubber transition state even at 293 K due to the surface segregation of chain end groups. Also, temperature-dependent LFM measurement revealed that the surface molecular motion of PS was activated compared with bulk one even though *M*n of the monodisperse PS was as high as 140 k. In the case of the polydisperse PS film, although the surface molecular motion was activated in comparison with bulk one, the change in surface dynamic viscoelastic characteristic of a glass–rubber transition state were not observed at 293 K. The difference in the activation for the surface molecular motion between the monodisperse and the polydisperse PS film can be explained on the basis of the difference in chemical structure of the chain end groups. Also, in the case of the broad molecular weight distribution, if lower molecular weight component was not present, the surface molecular motion was not activated at room temperature. The surface molecular motion at the P(St-b-MMA) film surface was evaluated on the basis of D-XPS. It was revealed that the surface molecular motion for the P(St-b-MMA) film was activated compared with that for its bulk sample. It was suggested that T_g of the P(St-b-MMA) film decreased with a decrease in distance from the outermost surface.

ACKNOWLEDGEMENTS

This work was partially supported by Grant-in-Aid for COE Research from Ministry of Education, Sports and Culture, and Grant from New Energy and Industrial Technology Development Organization (New Materials, A-068).

REFERENCES

1. Schrader, M. and Loeb, G., eds. *Modern Approaches to Wettability*. Plenum Press, New York, 1992.
2. Garbassi, F., Morra, M., Occhiello, E. *Polymer Surfaces from Physics to Technology*. Wiley, New York, 1994.
3. Keddie, J. L., Jones, R. A. L. and Coury, R. A., *Europhys. Lett.*, 1994, **27**, 49.
4. van Zanten, J. H., Wallace, W. E. and Wu, W. L., *Phys. Rev. E.*, 1996, **53**, R2053.
5. De Maggio, G. B., Frieze, W. E., Gidley, D. W., Zhu, M., Hristov, H. A. and Yee, A. F., *Phys. Rev. Lett.*, 1997, **78**, 1524.
6. Hall, D. B., Hooker, J. C. and Torkelson, J. M., *Macromolecules*, 1997, **30**, 667.
7. Forrest, J. A., Dalnoski-Veress, K., Stevens, J. R. and Dutcher, J. R., *Phys. Rev. Lett.*, 1996, **77**, 2002.
8. Mansfield, K. F. and Theodourou, D. N., *Macromolecules*, 1991, **24**, 6283.
9. Meyers, G. F., DeKoven, B. M. and Seitz, J. T., *Langmuir*, 1992, **8**, 2330.
10. Guntherodt, H. H. and Wiesendanger, R. *Scanning Tunneling Microscopy, Vols.I–III*. Springer, New York, 1992-1993.
11. Binnig, G., Quate, C. F. and Gerber, C. G., *Phys. Rev. Lett.*, 1986, **56**, 930.
12. Maivald, P., Butt, H. J., Gould, S. A. C., Prater, C. B., Drake, B., Gurley, J. A., Elings, V. B. and Hansma, P. K., *Nanotechnology*, 1991, **2**, 103.
13. Radmacher, M., Tillmann, R. W. and Gaub, E., *Biophys. J.*, 1993, **64**, 735.
14. Kajiyama, T., Tanaka, K., Ohki, I., Ge, S.-R., Yoon, J.-S. and Takahara, A., *Macromolecules*, 1994, **27**, 7932.
15. Tanaka, K., Taura, A., Ge, S.-R., Takahara, A. and Kajiyama, T., *Macromolecules*, 1996, **29**, 3040.
16. Kajiyama, T., Tanaka, K. and Takahara, A., *Macromolecules*, 1997, **30**, 280.
17. Naganuma, S., Sakurai, T., Takahashi, Y. and Takahashi, S., *Kobunshi Kagaku*, 1972, **29**, 105.
18. Overney, R. M., Meyer, E., Frommer, J., Guntherodt, H.-J., Fujihira, M., Takano, H. and Gotoh, Y., *Langmuir*, 1994, **10**, 1281.
19. Barger, W., Koleske, D., Feldman, K., Kruger, D. and Colton, R., *ACS Polym. Prep.*, 1996, **37**, 606.
20. Grosch, K. A., *Proc. R. Soc. London A*, 1963, **274**, 21.
21. Haugstad, G., Gladfelter, W. L., Weberg, E. B., Weberg, R. T. and Jones, R. R., *Langmuir*, 1995, **11**, 3473.
22. Hertz, H., *J. Reine Angew. Math.*, 1882, **92**, 156.
23. Kajiyama, T., Tanaka, K. and Takahara, A. *Macromolecules*, 1997, **30**, 6626.
24. Mayes, A. M., *Macromolecules*, 1994, **27**, 3114.
25. Kajiyama, T., Tanaka, K. and Takahara, A., *Macromolecules*, 1995, **28**, 3482.
26. Tanaka, K., Takahara, A. and Kajiyama, T., *Acta Polym.*, 1995, **46**, 476.
27. Tanaka, K., Takahara, A., and Kajiyama, T. *Macromolecules*, submitted for publication.
28. Kajiyama, T., Tanaka, K., and Takahara, A. *Bull. Chem. Soc. Jpn.*, 1997, **70**, 1491.
29. Koberstein, J. T., *MRS Bulletin*, 1996, **21**, 19.
30. Andrade, J. D., in *Surface and Interfacial Aspects of Biomedical Polymers Vol. 1—Surface Chemistry and Physics*, ed. J. D. Andrade. Plenum Press, New York, 1985.
31. Paynter, R. W., *Surf. Interface Anal.*, 1981, **3**, 186.
32. Wu, S. and Paul, D. R., eds. *Polymer Blends Vol. 1*. Academic Press, New York, 1978.
33. Ashley, J. C., *IEEE Trans. Nucl. Sci.* 1980, NS-27, 1454.
34. Tanaka, K., Takahara, A., and Kajiyama, T., unpublished data.
35. Liu, Y., Russell, T. P., Samant, M. G., Stohr, J., Brown, H. R., Cossy-Favre, A., and Diaz, J., *Macromolecules*, 1997, **30**, 7768.